EARTH ANTENNA TEMPERATURE VARIABILITY FOR CYGNSS

Mary Morris, David D. Chen, and Christopher S. Ruf

University of Michigan, Ann Arbor, MI, USA

ABSTRACT

Calibration algorithms are being developed for the CYclone Global Navigation Satellite System (CYGNSS) mission in anticipation of a late-2016 launch date. Antenna temperature (TA) of oceanic scenes will be used to confirm the relationship between receiver noise temperature and physical temperature—which will drift over time. In this work, we develop an open ocean TA model for CYGNSS to support the L1A calibration process. This model needs to be as simple as possible, while still meeting accuracy requirements. We show that, for purposes of the CYGNSS L1A calibration, it is possible to use a single value of TA = 99.4 K, within the 2 K accuracy requirement.

Index Terms— CYGNSS, microwave radiometry, calibration

1. INTRODUCTION

The CYclone Global Navigation Satellite System (CYGNSS) constellation of eight, small satellites, to be launched in late 2016, will provide unique observations of ocean surface wind speed under all precipitating conditions [1]. In preparation for launch, calibration algorithms are being developed. During the L1A calibration process, antenna temperature (TA) is used to confirm the relationship between receiver noise temperature and physical temperature. The receiver noise temperature depends on the receiver physical temperature; this relationship will drift over time. There is a model for this time-dependent drift and this model can be verified with CYGNSS observations over open-ocean. The verification process requires that a TA model be developed for CYGNSS, to serve as a simulation of CYGNSS TA. The objective of this work is to develop a CYGNSS TA model that is as simple as possible, within a 2 K accuracy requirement.

2. ANCILLARY DATA

Ancillary data are needed as input to the radiative transfer model (RTM) which forms the basis for the TA calculation. In order to explore the earth brightness variability that would be expected over seasonal and diurnal time scales, data were acquired from the NCEP Climate System Reanalysis [2] for 00, 06, 12, and 18 UTC for the first day of every month of 2009. These NCEP data were input into the RTM to simulate observations of left-hand circularly polarized (LHCP) TB at 1.57542 GHz.

3. RADIATIVE TRANSFER MODEL

Top-of-atmosphere (TOA) TB can be modeled with

$$TB = e^{-\tau}\left(1-\varepsilon\right)\left[TB_{DN} + e^{-\tau}TB_{COS}\right] + e^{-\tau}\varepsilon T_{SFC} + TB_{UP} \quad (1)$$

where $e^{-\tau}$ is the atmosphere transmissivity, ε is the ocean surface emissivity, TB_{UP} and TB_{DN} are the upwelling and downwelling atmosphere TB, T_{SFC} is the sea surface temperature, and TB_{COS} is the cosmic microwave background TB. Atmospheric absorption is modeled for water vapor [3], O_2, and N_2 [4-5]. Ocean surface emissivity depends on sea surface temperature, sea surface salinity, surface wind speed, frequency, and polarization. All of these variables, except wind speed, can be accounted for with the emissivity models of Meissner and Wentz [6] and Elsaesser [7]. Wind-driven LHCP excess emissivity at L-band can be modeled based on [12].

TB depends on a variety of instrument and environmental parameters. Figure 1 shows TB dependence on instrument related parameters like polarization and earth incidence angle (EIA). One important point to take away from Fig.1 is that LHC polarized TB changes more slowly than H and V pol TB with increasing EIA. This fact impacts the calibration of CYGNSS data, which operates with LHCP.

Figure 2 shows TB dependence on a few environmental parameters at the CYGNSS L-band operating frequency, 1.57542 GHz, at nadir (0˚ EIA). Note that there is very little sensitivity to water vapor. However, the surface variables of sea surface salinity (SSS) and sea surface temperature (SST) have comparatively stronger signatures in L-band TB.

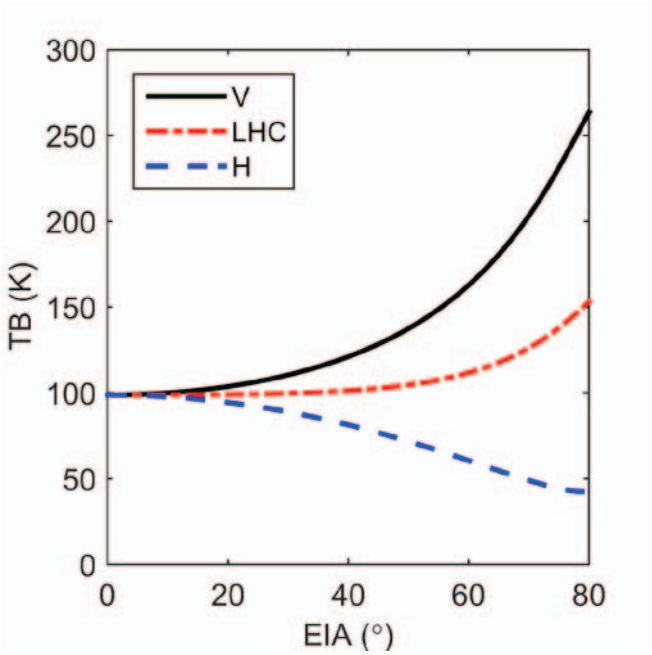

***Figure 1**: A comparison of the TB dependence over a range of earth incidence angles (EIA) for vertical (V), horizontal (H), and left-hand circular (LHC) polarizations. These TB calculations at 1.57542 GHz are based on an atmosphere profile with surface temperature = 288.15 K, sea surface salinity = 35 ppt, surface absolute humidity = 15 g m^{-3}, surface wind speed = 0, surface pressure = 1013.25 mb.*

In order to develop a faster RTM, and due to the lack of atmosphere sensitivity at L-band, the atmospheric contributions to the TOA TB were parameterized. These simplifications were employed after studying the variability of the L-band LHCP TB for all 00 UTC oceanic ancillary data described in section 2. The first suitable parameterization is the use of an average upwelling TB, downwelling TB, and optical depth, instead of a set of separately calculated values for each TB simulated. For the parameterized RTM, upwelling TB, downwelling TB, and optical depth is assumed to be the average of all of those parameters calculated using the 00 UTC ancillary dataset; these values are reported in Table 1.

Figure 3 shows evidence for using an average upwelling and downwelling TB as well as optical depth (τ) for all further analysis. The Fig.3 histograms show upwelling TB, downwelling TB, and optical depth (τ) calculated with the atmospheric absorption models mentioned previously, for the 00 UTC NCEP reanalysis data at 0º Earth incidence angle (EIA). Also labeled in Fig.3 are the average (dashed red line, μ) and standard deviation (σ) of the parameters. The variance of these parameters is much lower than the 2 K accuracy requirement, so the average of all of these parameters is used for the parameterized version of the RTM used in the simulation of CYGNSS TA.

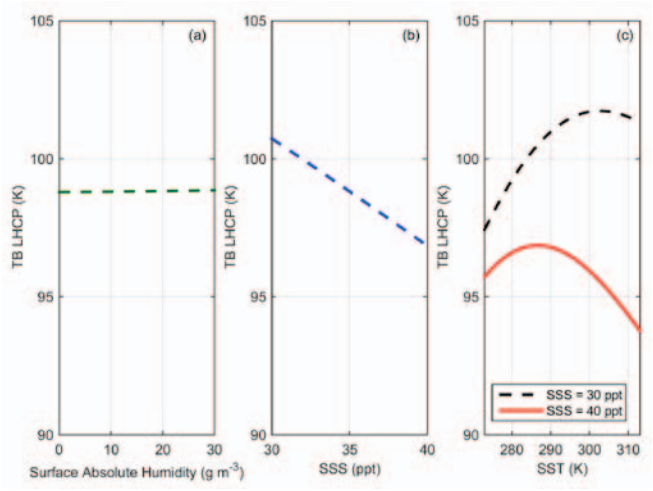

***Figure 2:** Typical values of left-hand circular polarized (LHCP) brightness temperature (TB) over a variety of environment input. In all 3 subplots, frequency = 1.57542 GHz, earth incidence angle = 0 degrees, and surface wind speed = 0 m s^{-1}. The atmosphere is modeled with typical profiles of temperature and pressure, where the surface layer air temperature = 288.15 K and the surface pressure is 1013.25 hPa. In Fig.3.a, sea surface salinity (SSS) and temperature (SST) are held constant (35 ppt, 288.15 K, respectively), and the absolute humidity at the surface is allowed to vary. In Fig.3.b, SST and surface absolute humidity are held constant (288.15 K, 15 g m^{-3}, respectively), and the SSS is allowed to vary. In Fig.3.c, SST is allowed to vary for two sets of SSS, while keeping surface absolute humidity constant at 15 g m^{-3}.*

***Table 1:** The constant values of upwelling TB (TB_{UP}), downwelling TB (TB_{DN}), and optical depth used in the parameterized CYGNSS RTM*

Parameter	CYGNSS RTM Constant Value
TB_{UP} (K)	2.0053
TB_{DN} (K)	2.0060
Optical Depth (Np)	7.6 x 10^{-3}

The second suitable parameterization is a parameterized EIA dependence. Slant path integration through the atmosphere is parameterized with

$$TB_{UP}(\theta) = \sec(\theta) TB_{UP}(\theta = 0^{\circ}) \qquad (2)$$

where θ is EIA and TB_{UP} is the upwelling TB at nadir (EIA = 0˚). Figure 4 shows evidence that the full integration along a slant path of the atmosphere can be simplified to (2). The black circles show the exact TB_{UP} calculated with the full integration along the slant path, then normalized with the corresponding TB_{UP} at nadir (0˚ EIA). The red line shows

the sec(θ) dependence. Since the red line goes through the black circles, all off-nadir upwelling or downwelling TB can be based on (2). To apply (2) to the downwelling TB, just replace the upwelling TB terms with the downwelling TB terms. These parameterizations speed up the RTM within the 2 K accuracy requirement.

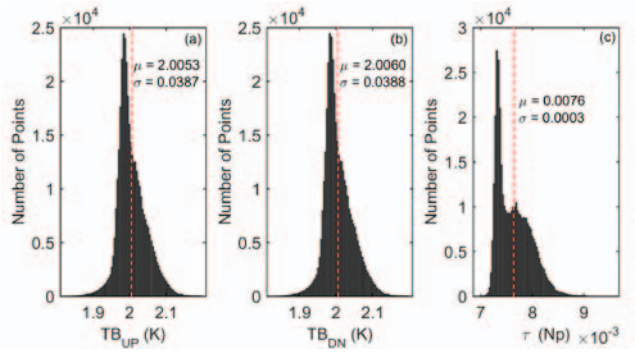

Figure 3: *(a) Upwelling Brightness Temperature (TB_{UP}) calculated at 0˚ EIA with all of the 00 UTC NCEP data. (b) Downwelling Brightness Temperature (TB_{DN}) calculated at 0˚ EIA with all of the 00 UTC NCEP data. (c) Optical depth (τ) calculated at 0˚ EIA with all of the 00 UTC NCEP data. Also labeled in these plots are the average (μ) (dashed red line) and the standard deviation (σ) for all parameters.*

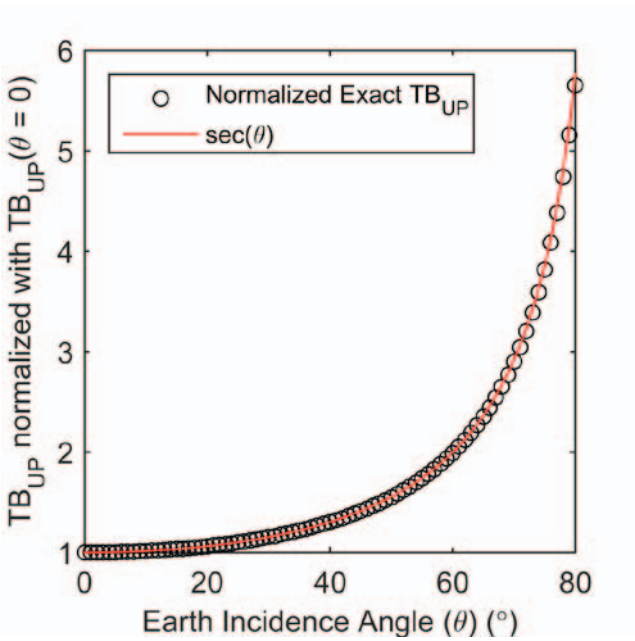

Figure 4: *Black circles: Upwelling brightness temperature (TB_{UP}) normalized with the nadir ($\theta = 0°$) value of TB_{UP} and calculated over a range of earth incidence angles using the full radiative transfer model. The red line shows sec(θ) to show that the downwelling and upwelling TB can be approximated at off-nadir values by multiplying the nadir value with sec(θ).*

Using the RTM described above, we can then calculate the TA using

$$TA = \frac{1}{\Omega_A} \iint_{4\pi} TB_{ALL}(\theta_a) P(\theta_a, \phi) d\Omega \tag{3}$$

where TB_{ALL} is defined depending on whether the field of view is above or below the horizon as

$$TB_{ALL} = \begin{cases} TB(\theta_i(\theta_a)) & 0 \le \theta_a < \theta_s \\ 2.7K & \theta_s \le \theta_a \le 180^\circ \end{cases} \tag{4}$$

and θ_a is the antenna off-nadir angle, θ_i is the earth incidence angle corresponding to θ_a, θ_s is the angle where the antenna is looking out to space (where θ_i becomes undefined), $P(\theta_a, \phi)$ is the antenna power pattern for azimuth angle ϕ, and Ω_A is the solid angle of the antenna pattern.

4. RESULTS

The appropriate CYGNSS TA model depends on the variability of TA. TA was calculated using a parameterized RTM, using all NCEP data summarized in section 2. However, due to time limitations, TA was only calculated on a 5˚ × 5˚, (open) Pacific Ocean grid. The typical variability is summarized visually in Fig.5. Figure 5a is a histogram of all the CYGNSS TA, with the mean (red dashed line, μ) and standard deviation (σ) labeled. Figure 5b is the same CYGNSS TA data, but in box plot form, for comparison to subplots (c-e). Figure 5c separates the TA dataset by southern (SH) and northern (NH) hemispheres. Figure 5d separates the TA dataset out by hour of the day. Figure 5e separates the TA dataset by month. There is not a lot of variability in these separations. Seasonal and spatial variations are both larger than diurnal variations. The average TA is 99.4 K, with a standard deviation of 0.75 K.

5. CONCLUSIONS

The analysis above allows us to choose the simplest TA model possible within the 2 K accuracy requirement. The mean TA value, 99.4 K, will be used as the CYGNSS TA, independent of latitude, longitude, time of day, day of year, or any other parameters. For purposes of the CYGNSS L1A calibration, it is possible to use a single value of TA because the RMSE of the TA dataset analyzed is 0.75 K, which is within the 2 K accuracy requirement. This uncertainty includes changes with location, season, and diurnal dependence.

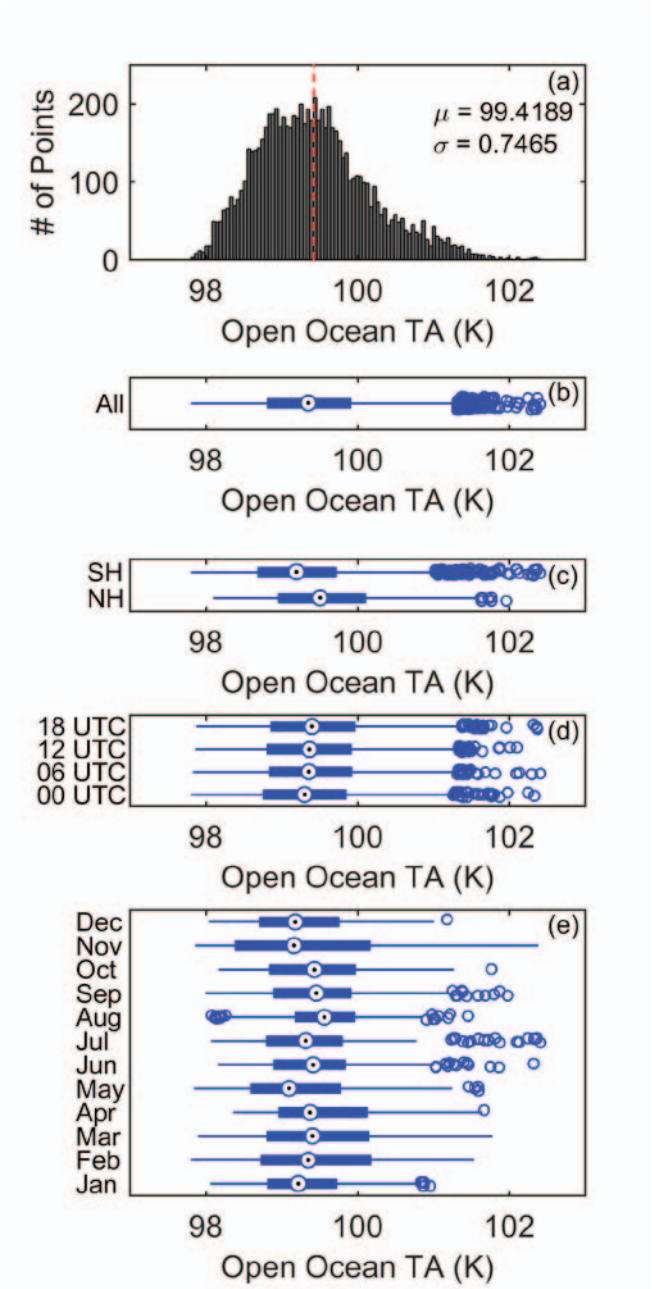

Figure 5: *(a) Histogram of all open ocean TA calculated for the Pacific Ocean using NCEP data. (b) Boxplot of the data plotted in (a). (c) TA boxplot separated by northern (NH) and southern (SH) hemisphere. (d) TA boxplot separated by hour of the day. (e) TA boxplot separated by month.*

6. REFERENCES

[1] C. Ruf, R. Atlas, P. Chang, M.P. Clarizia, J. Garrison, S. Gleason, S. Katzberg, Z. Jelenak, J. Johnson, S. Majumdar, A. O'Brien, D. Posselt, A. Ridley, R. Rose and V. Zavorotny, "New Ocean Winds Satellite Mission to Probe Hurricanes and Tropical Convection," *Bulletin of American Meteorological Society (BAMS)*, doi:10.1175/BAMS-D-14-00218.1, Apr 2016.

[2] S. Saha, et al. (2010) NCEP Climate Forecast System Reanalysis (CFSR) 6-hourly Products, January 1979 to December 2010. Research Data Archive at the National Center for Atmospheric Research, Computational and Information Systems Laboratory. http://dx.doi.org/10.5065/D69K487J. Accessed† 07 Nov 2015.

[3] P. Rosenkranz, "Water vapor microwave continuum absorption: A comparison of measurements and models," *Radio Sci*., vol. 33, no. 4, pp. 919–928, 1998.

[4] H. J. Liebe, P.W. Rosenkranz, and G. A. Hufford, "Atmospheric 60-GHz oxygen spectrum: New laboratory measurements and line parameters," *J. Quant. Spectrosc. Radiat. Transf.*, vol. 48, pp. 629–643, 1992.

[5] P. W. Rosenkranz, "Absorption of microwaves by atmospheric gases," in *Atmos. Remote Sensing by Microwave Radiometry*, M. A. Janssen, Ed. Hoboken, NJ: Wiley, 1993, p. 37.

[6] T. Meissner and F. J.Wentz, "The complex dielectric constant of pure and sea water from microwave satellite observations," *IEEE Trans. Geosci. Remote Sens*., vol. 42, no. 9, pp. 1836–1849, Sep. 2004.

[7] G. Elsaesser, "A parametric optimal estimation retrieval of the non-precipitating parameters over the global oceans," M.S. thesis, Colorado State Univ., Fort Collins, CO, 2006.

[8] N. Reul, J. Tenerelli, B. Chapron, D. Vandemark, Y. Quilfen, and Y. Kerr, "SMOS satellite L-band radiometer: A new capability for ocean surface remote sensing in hurricanes," *J. Geophys. Res.–Oceans*, vol. 117, no. C2, pp. C02006-1–C02006-24, Feb. 2, 2012.